International Journal of Thermofluid Science and Technology (2021)
Volume 8, Issue 1, Paper No. 080103
https://doi.org/10.36963/IJTST.2021080103
Research Article

Effects of magnetic field on blood flow with suspended copper nanoparticles through an artery with overlapping stenosis

C. Umadevi [1], G. Harpriya[2], M. Dhange[3,*], G. Nageswari[4]

[1]*Department of Mathematics, T.K.R. College of Engineering and Technology, Hyderabad, India*
[2]*Department of Mathematics, Gates Institute of Technology, Gooty, India*
[3]*Department of Mathematics, B.L.D.E.A's V.P. Dr. P.G. Halakatti College of Engineering and Technology, Vijayapur, India*
[4]*Department of Mathematics, PVKK Institute of Technology, Anantapur, India*

Received: 9 December 2020; Received in revised form: 19 January 2021; Accepted: 23 February 2020; Published online 10 March 2021

Abstract

The flow of blood mixed with copper nanoparticles in an overlapping stenosed artery is reported in the presence of a magnetic field. The presence of stenosis is known to impede blood flow and to be the cause of different cardiac diseases. The governing nonlinear equations are rendered dimensionless and attempted under the conditions of mild stenosis. The analytical solutions for velocity, resistance to the flow, wall shear stress, temperature, and streamlines are obtained and analyzed through graphs. The obtained outcomes show that the temperature variation in copper nanoparticles concentrated blood is more and flow resistance is less when compared to pure blood. The investigations reveal that copper nanoparticles are effective to reduce the hemodynamics of stenosis and could be helpful in biomedical applications.

Keywords: Magnetic field, overlapping stenosis, copper nanoparticles, wall shear stress.

1. Introduction

Microvessels have a very significant role in the hemostasis of organs and tissues. Blood flows through them and delivers oxygen and nutrients to the organs, where they are exchanged with carbon oxides and metabolic wastes. In all cases, the chemical carriers are the red blood cells (RBCs). In terms of hemodynamics, about 80% of the total pressure drop of the circulation takes place in microvessels. Popel and Johnson [1] and Lipowsky [2] were studied the microvascular rheology and hemodynamics of blood. Freund [3] analyzed the flowing blood cells through numerical simulation because of their small diameter ($\leq$300 μm) which is comparable to that of RBCs ($\leq$8 μm). This has many implications on the flow field: the velocity profiles are not parabolic, the apparent viscosity is not constant and depends on the vessel diameter, the hematocrit is also dependent on the vessel diameter, phase separation occurs at bifurcations and a cell-free layer is formed along the wall (Sharan and Popel [4]).

**Corresponding e-mail*: math.mallinath@bldeacet.ac.in (M. Dhange)

Blood consists of a concentrated suspension of blood cells in plasma. Of the formed elements, the white blood cells together with the platelets occupy less than one percent of the volume of blood, while the RBCs form the dominant matter of blood, occupying about 45% and 40% of the volume for men and women, respectively (Chien et al. [5]). Zixiang-Liu et al [6] investigated the nanoparticle movement in cellular blood flow. Thus, the rheological properties of blood are primarily governed by the concentration of RBCs and their behavior at different shear rates. As the blood flows through microtubes, non-Newtonian effects, such as shear-thinning and viscoelasticity, become more important (Thurston [7]). Several constitutive models for the stresses of the model have been developed to present the viscoelastic, shear-thinning character as well as the non-homogeneous phenomena of blood flow (Apostolidis and Beris [8]). Quemada [9] derived a generalized Maxwell constitutive model by assuming that aggregation and disaggregation are simple relaxation processes and developed a relation between the number fraction of red blood cells in aggregates and the mean relaxation times of aggregation and disaggregation. Williams et al. [10] also derived a Maxwell model, based on quite a few restrictions, including that flow conditions, are near equilibrium. Vlastos et al. [11] examined viscoelastic effects and proposed a Carreau model for the description of blood shear-thinning (see also Dimakopoulos et al. [12]). Anand et al. [13] proposed a viscoelastic model that is based on the thermodynamic framework developed by Rajagopal and Srinivasa [14]. The model accounts for the dependence of the relaxation times on the shear rate and is in good agreement with experimental data in steady Poiseuille flow and oscillatory flow (Bodnar and Sequeira [15]). Chakraborty et al. [16] evaluated three viscoelastic models for the simulation of blood flow in a two-dimensional collapsible channel. This was one of the first studies in fluid-structure interaction with a viscoelastic assumption for blood rheology.

The term stenosis indicates the constricting of the artery because of the growth of the atherosclerotic deposition or different sorts of anomalous tissue development. As the development ventures into the lumen (depression) of the artery, blood flow is impeded. The impediment may harm the inner cells of the wall and may prompt further development of the stenosis. In this way, there is a coupling between the development of stenosis and the flow of blood in the artery since every influence the other. The advancement of stenosis in an artery can have genuine outcomes and can disturb the typical working of the circulatory system. Blood flow is an eminent topic to researchers due to its huge applications in arterial mechanics. The study of blood flows in a stenosed blood vessel plays a significant role to inspect the different types of heart diseases. Robert [17] studied the dynamics of blood flow in stenotic lesions. Stenosis was first studied by Young [18]; who claims that very small growth leading to mild stenosis obstructions. Misra et al. [19] and Chakravarthy and Mandal [20] explored the blood flow through tapered overlapping arteries using a non-Newtonian fluid model. Because of its importance, Ponalagusamy [21], Reddy et al. [22], Sahu et al. [23], and Nadeem et al. [24] have studied the behavior of blood flow in the stenosed artery by assuming blood as Newtonian or Non-Newtonian fluid. Hemodynamics in stenotic vessels of small diameter under steady-state conditions and effects of viscoelasticity and migration of red blood cells were studied by Dimakopoulos et al. [25] and observed that the viscoelastic effects in blood flow were found to be responsible for steeper decreases of the tube and discharge hematocrits as a decreasing function of concentration ratio. Stenosis may form in different shapes like multiple, overlapping, or irregular shapes. A mathematical model of non-Newtonian blood flow in a tapered overlapping constriction is investigated by Ismail et

al [26] and explored the occurrence of overlapping constriction by the power-law model of blood flows. Srivastava et al. [27] studied the Non-Newtonian effects on blood flows in overlapping stenosis. Shit et al. [28] developed a numerical model of the pulsatile blood flow in a porous overlapping abnormality under influence of magnetic fields.

Nanotechnology plays a prominent role in branch fluid dynamics. It has huge applications: medicines, chemicals, food, automobiles, etc. A homogeneous mixture of nanoparticles consists of base fluids are known as nanofluids. The nanoparticles are made of oxides, metals, carbides, and carbon nanotubes. A base fluid contains oil, ethylene glycol, and water. Nanofluid has several biological applications such as probing of DNA structure, protein detection, cancer therapy, etc. The nanofluid was first proposed by Chio [29]. Nanofluids can be enhanced by thermophysical properties compared to ordinary fluids. Buongiorno [30] studied the abnormal convective heat transfer enhancement in nanofluids. Vajravelu et al. [31] clearly show the variations in convective heat transfer in the flow of Ag-blood and Cu-water nanofluids over a stretching surface. Gudekote et al. [32], Sankad and Dhange [33] investigated the impact of wall features, chemical reactions, and variable viscosity on the peristaltic flow of Newtonian and Jeffrey fluid in a curved channel. The impact of non-uniform heat source/sink and variable viscosity on the mixed convection flow of third-grade nanofluid over an inclined stretched Riga plate was investigated by Nayak et al. [34]. Larimi et al. [35] and Shaw et al [36] explored the numerical simulation of magnetic nanoparticles/drug targeting in a bifurcation and permeable vessel/microvessel.

Several researchers ([37-43]) studied the nanoparticle suspended fluid flow and showed that this technique will enable us to get appropriate results when these kinds of problems are modeled. According to some authors, the Ag-water solution decreases the boundary layer thickness than the Cu - water solution.

The advancement of stenosis in an artery can have genuine outcomes and can disturb the typical working of the circulatory system. Specifically, it might prompt: increased resistance to flow with a possible serious decrease in blood flow, increased risk of complete occlusion, abnormal cell development in the region of the stenosis. Due to its importance, Ramana et al. [44] studied the simulation of temperature and concentration dispersion in a couple stress nanofluid flows through stenotic tapered arteries. Nadeem and Ijaz [45] investigated the impact of nanoparticles on the blood flow of a tapered catheterized elastic artery with overlapping stenosis. The Cu-blood flow model through a catheterized mild stenotic artery with thrombosis was explored by Elnaqeeb et al. [46]. Akbar and Butt [47] and Akbar [48] investigated the effect of a magnetic field and permeable walls on copper suspended nanofluid through composite arteries and its applications in nanomedicines.

The issue considered in the current research work has potential in engineering and biomedical applications. In the literature review, it is observed that many investigators have worked on the stenosed artery. However, no investigation has demonstrated the effect of the magnetic force on blood mixed with copper nanoparticles in the overlapping stenosed artery. The pressure droplet, flow resistance, and shear-stress at the wall are analyzed and the special effects of many significant constraints are observed through the graphs. The thermophysical properties of blood and copper nanoparticles are shown in Table 1.

Table 1. Thermophysical properties of blood and nanoparticles (Pak and Cho [49])

Materials	Copper	Blood

Symbols	Cu	-
$\rho\ (kg/m^3)$	8933	1063
$c_p(J/kg\ K)$	385	3594
$K(W/m\ K)$	400	0.492
$\gamma\ x\ 10^{-5}\ (K^{-1})$	1.67	0.18

Nomenclature

(u, v)	velocity components in (r, z) directions (m/s)	$R(z)$	the radius of the tube at the stenotic region (m)
T, θ	the temperature of the fluid (K)	$R_0(z)$	the radius of the tube at the non-stenotic region (m)
Q_0	Heat absorption or heat generation constraint $(J/kg\ K)$	d	the beginning distance of the stenotic region (m)
μ_{nf}	dynamic viscosity (kg/ms)	L	length of the tube (m)
ρ_{nf}	Density (kg/m^3)	L_0	length of the stenotic region (m)
k_{nf}	thermal conductivity $(W/m\ K)$	δ	height of the stenosis (m)
α_{nf}	thermal diffusivity (m^2/s)	g	gravitational acceleration (m/s^2)
$(\rho c_p)_{nf}$	heat capacitance of the nanofluid $(J/kg\ K)$	p	pressure (kg/ms^2)
β	heat source or sink constraint $(J/kg\ K)$	$\bar{\lambda}$	resistance to flow (kg/m^4s)
τ_h	wall shear stress (N/m^2)	M	magnetic field constraint
q	volume flow rate (kW/m^2)	G_r	Grashof number

2. Mathematical formulation and its solution

Let us consider an incompressible and axisymmetric flow of blood mixed with copper nanoparticles through a tube having overlapping stenosis in the presence of a uniform transverse magnetic field (cf. Fig. 1).

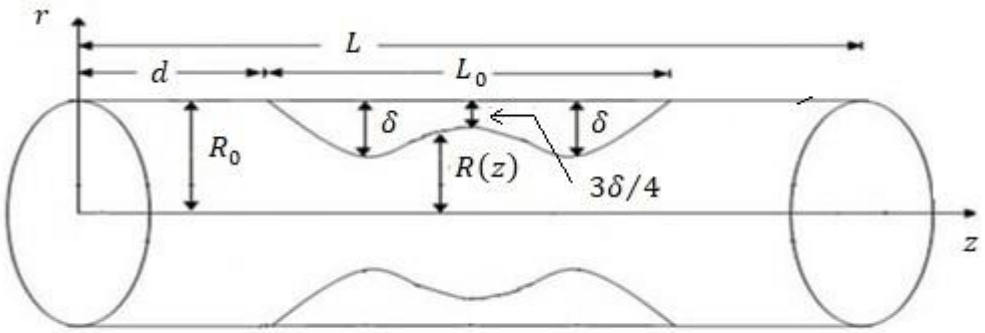

Fig1. Schematic presentation of the hose with stenosis

The geometry of the artery wall having stenosis can be described as (Chakravarty and Mandal [20]):

$$h = \frac{R(z)}{R_0} = \begin{cases} 1 - \frac{3\delta}{2R_0 L_0^4}\left[11(z-d)L_0^3 - 47(z-d)^2 L_0^2 + 72(z-d)^3 L_0 - 36(z-d)^4\right] & : d \le z \le d + L_0 \\ 1 & : \text{otherwise} . \end{cases} \tag{1}$$

Here $R(z)$ is the tube radius at the stenotic region and $R_0(z)$ is the radius in the non-stenotic region, d is the beginning of the stenotic region, L is the length of the tube L_0 is the length of the stenotic region, δ is the maximum height of the stenosis at $z = d + \frac{L_0}{6}$, $z = d + \frac{5L_0}{6}$, and $\frac{3\delta}{4}$ is the critical height of the stenosis at $z = d + L_0/2$, from the origin.

The governing equations of an incompressible nanofluid (Akbar and Butt [47]) can be specified as:

$$\frac{\partial v}{\partial r} + \frac{v}{r} + \frac{\partial u}{\partial z} = 0 \tag{2}$$

$$\rho_{nf}\left(v\frac{\partial v}{\partial r} + u\frac{\partial v}{\partial z}\right) = -\frac{\partial p}{\partial r} + \mu_{nf}\frac{\partial}{\partial r}\left(2\frac{\partial v}{\partial r}\right) + \mu_{nf}\frac{\partial}{\partial z}\left(2\frac{\partial v}{\partial z} + \frac{\partial u}{\partial r}\right) \tag{3}$$

$$\rho_{nf}\left(v\frac{\partial u}{\partial r} + u\frac{\partial u}{\partial z}\right) = -\frac{\partial p}{\partial z} + \mu_{nf}\frac{\partial}{\partial z}\left(2\frac{\partial u}{\partial z}\right) + \frac{\mu_{nf}}{r}\frac{\partial}{\partial r}\left[r\left(\frac{\partial v}{\partial z} + \frac{\partial u}{\partial r}\right)\right] - g\rho_{nf}\alpha(T - T_0) - \sigma B_0^2 u \tag{4}$$

$$\left(v\frac{\partial T}{\partial r} + u\frac{\partial T}{\partial z}\right) = \frac{K_{\eta f}}{(\rho c_p)_{\eta f}}\left(\frac{\partial^2 T}{\partial r^2} + \frac{1}{r}\frac{\partial T}{\partial r} + \frac{\partial^2 T}{\partial z^2}\right) + \frac{Q_0}{(\rho c_p)_{\eta f}} \tag{5}$$

The boundary conditions are well-defined as:

$$\frac{\partial u}{\partial r} = 0, \quad \frac{\partial T}{\partial r} = 0 \quad \text{at} \quad r = 0 \tag{6}$$

$$u = 0, \quad T = 0 \quad \text{at} \quad r = h \tag{7}$$

Here, u, v are the velocity components in r and z directions, respectively, T is the temperature of the fluid, and Q_0 is heat absorption or heat generation parameter.
The effective dynamic viscosity (μ_{nf}), effective density (ρ_{nf}), effective thermal conductivity (k_{nf}), thermal diffusivity (α_{nf}), and the heat capacitance $(\rho c_p)_{nf}$ of the nanofluids, respectively, are specified ([30 - 31]) as follows:

$$\mu_{nf} = \frac{\mu_f}{(1-\varphi)^{2.5}}, \qquad \rho_{nf} = (1-\varphi)\rho_f + \varphi\rho_f, \quad k_{nf} = k_f \left\{ \frac{k_s + 2k_f - 2\varphi(k_f - k_s)}{k_s + 2k_f + 2\varphi(k_f - k_s)} \right\}$$

$$\alpha_{nf} = \frac{k_{nf}}{(\rho c_p)_{nf}}, \qquad (\rho c_p)_{nf} = (1-\varphi)(\rho c_p)_f + \varphi(\rho c_p)_f$$

The scaling variables are as stated:

$$\bar{r} = \frac{r}{R_0}, \quad \bar{z} = \frac{z}{L_0}, \qquad \bar{u} = \frac{u}{U}, \quad \bar{\upsilon} = \frac{L_0}{\delta U}\upsilon, \quad \bar{d} = \frac{d}{L_0}, \qquad \bar{R} = \frac{R}{R_0}, \qquad \bar{p} = \frac{UL_0\mu}{R_0^2}p$$

$$M^2 = \frac{\sigma B_0^2 R_0^2}{\mu_f}, \quad G_r = \frac{g\alpha R_0^2 T_0 \rho_{nf}}{U\mu_f}, \qquad \bar{\delta} = \frac{\delta}{R_0}, \theta = \frac{T - T_0}{T_0}, \qquad \beta = \frac{Q_0 R_0^2}{k_f T_0}. \tag{8}$$

Here U is the averaged velocity over the section of the tube with a radius R_0.

Applying the above scaling variables of Eq. (8) in Eqs. (2) - (5) along with mild stenosis $\left(\frac{\delta}{R_0} \ll 1\right)$ condition $\epsilon = \frac{R_0}{L_0} = o(1)$, and after dropping the dashes we get as:

$$\frac{\partial p}{\partial r} = 0 \tag{9}$$

$$\frac{dp}{dz} = \frac{1}{(1-\varphi)^{2.5}} \frac{1}{r}\frac{\partial}{\partial r}\left(r\frac{\partial u}{\partial r}\right) - M^2 u + G_r\theta \tag{10}$$

$$\frac{1}{r}\frac{\partial}{\partial r}\left(r\frac{\partial \theta}{\partial r}\right) + \beta\left(\frac{k_{nf}}{k_f}\right) = 0 \tag{11}$$

Using scaling variables in the boundary conditions of temperature and velocity for artery wall, and are given as:

$$\frac{\partial u}{\partial r} = 0, \quad \frac{\partial \theta}{\partial r} = 0 \quad \text{at} \quad r = 0, \tag{12}$$

$$u = 0, \quad \theta = 0 \quad \text{at} \quad r = h. \tag{13}$$

Where M is the magnetic field constraint, β is the heat absorption constraint, θ is the temperature, and G_r is the Grashof number.

The velocity of a fluid with copper nanoparticle suspension and temperature are obtained by solving the Eqs. (10) And (11) of the model along with the boundary conditions (12, 13), and are given below as:

$$u = \left\{\frac{\frac{1}{M^2}\frac{dp}{dz} - \frac{G_r\beta}{M^2}\left(\frac{k_f}{k_{nf}}\right) - \frac{1}{M^2}\frac{Sin\,\alpha}{F}}{I_0\left(Mh\sqrt{(1-\varphi)^{2.5}}\right)}\right\} I_0\left(Mr\sqrt{(1-\varphi)^{2.5}}\right) - \frac{G_r\beta}{4M^2}\left(\frac{k_f}{k_{nf}}\right)(r^2-h^2) - \frac{1}{M^2}\frac{dp}{dz} + \frac{G_r\beta}{M^2}\left(\frac{k_f}{k_{nf}}\right) \tag{14}$$

$$\theta = \frac{-\beta}{4}\left(\frac{k_f}{k_{nf}}\right)(r^2-h^2) \tag{15}$$

Some of the important dimensional physical quantities are presented below. The flow rate q is given by

$$q = 2\int_0^h rudr. \tag{16}$$

$$q = \left(\frac{\frac{1}{M^2}\frac{dp}{dz} - \frac{G_r\beta}{M^2}\left(\frac{k_f}{k_{nf}}\right)}{I_0\left(Mh\sqrt{(1-\varphi)^{2.5}}\right)}\right)\left(\frac{hI_1\left(Mh\sqrt{(1-\varphi)^{2.5}}\right)}{M\sqrt{(1-\varphi)^{2.5}}}\right) + \frac{G_r\beta}{16M^2}\left(\frac{k_f}{k_{nf}}\right) + \frac{G_r\beta h^2}{2M^2}\left(\frac{k_f}{k_{nf}}\right) - \frac{h^2}{M^2}\frac{dp}{dz}$$

This gives us:

$$\frac{dp}{dz} = \frac{q - \frac{G_r\beta}{16M^2}\left(\frac{k_f}{k_{nf}}\right) - \frac{G_r\beta h^2}{2M^2}\left(\frac{k_f}{k_{nf}}\right) + \frac{G_r\beta}{M^2}\left(\frac{k_f}{k_{nf}}\right)\left(\frac{hI_1\left(Mh\sqrt{(1-\varphi)^{2.5}}\right)}{I_0\left(Mh\sqrt{(1-\varphi)^{2.5}}\right)M\sqrt{(1-\varphi)^{2.5}}}\right)}{\frac{-h^2}{2M^2} + \frac{h}{M^3}\left(\frac{I_1\left(Mh\sqrt{(1-\varphi)^{2.5}}\right)}{I_0\left(Mh\sqrt{(1-\varphi)^{2.5}}\right)\sqrt{(1-\varphi)^{2.5}}}\right)} \tag{17}$$

The pressure drop over one wavelength $p(0) - p(\lambda)$ is given by:

$$\Delta p = -\int_0^1 \frac{dp}{dz}\, dz. \tag{18}$$

The impedance is denoted by λ and is defined by:

$$\lambda = \frac{\Delta p}{q}. \tag{19}$$

The pressure drop in the normal portion of the artery at $h = 1$ is given by:

$$\Delta p_n = \left[-\int_0^1 \frac{dp}{dz}\, dz\right]_{h=1.} \tag{20}$$

The flow resistance directly impacts the stream of blood and has a direct connection with the flow rate of blood. The impedance within the normal artery may be computed as:

$$\lambda_n = \frac{\Delta p_n}{q}. \tag{21}$$

The normalized impedance can be calculated as:

$$\bar{\lambda} = \frac{\lambda}{\lambda_n}. \tag{22}$$

The shear stress on blood vessel walls is one of the physical quantities which have a significant influence on the flow of fluid at the wall. The wall shear-stress may be computed by using the formula:

$$\tau_h = -\frac{h}{2}\frac{dp}{dz}. \tag{23}$$

4. Discussion of outcomes

To comprehend the physiological behaviors of relevant constraints, the analytical expressions obtained in the preceding section are presented through graphs. The effects of various constraints (cf. height of stenosis, a radius of the tube, length of the tube, the length of a stenosis, heat source or sink parameters (β) on temperature) are involved, in the equations of temperature (θ), impedance $(\bar{\lambda})$ and wall shear stress (τ_h) have been carried out by *MATHEMATICA* software and entire results are presented in Fig. 2-12.

The effects of stenosis height (δ) and a heat source or sink constant (β) on temperature are shown in Figs.2-3. The temperature rises when the stenosis height and heat absorption constant (β) upturns. The temperature is higher in the middle of the tube and lowers near the walls. It is also noticed that the temperature deviation in blood mixed with copper nanoparticles is more than that of the pureblood.

Figures 4 - 6 illustrate the deviation in velocity (u) with that of the radial distance (r) for different values of stenosis height (δ), heat source or sink constant (β), Grashof number (G_r). It is experiential that the velocity of blood is high in the middle of the tube and decreases towards the wall, and the velocity is zero at the wall of the tube. It is also seen that the velocity rises to the stenosis height (δ), heat source or sinks constant (β), Grashof number (G_r), It is noticed that the rate of change in velocity is more in the case of copper nanoparticles contained blood due to features of nanoparticles. It clears that the magnitude of velocity is greater in the normal artery as compared with the stenosed artery. Furthermore, velocity attains higher values for diverging tapering as compared to converging tapering. The velocity is more when Cu nanoparticle concentration is increased in the blood, which means that the Cu nanoparticles can improve the blood velocity in the stenosed artery due to the high thermal conductivity of Cu nanoparticles. These results validate the outcomes of Akabar and Batt [47]. Magnetic forces are used for the transport, separation, positioning, and sorting of magnetic and non-magnetic objects. Many areas in microfluidic applications involve the manipulation of particles in a controllable manner. The effect of magnetic field constraint $(M)$is observed through Fig. 7. As an increase in magnetic field constraint (M) the velocity of blood decreases. It confirms the fact that the Lorentz force acts as a retarding force. Due to the influence of the magnetic field, most of the nanoparticles and iron particles of blood activates and it affects the velocity of blood flow in an artery. These outcomes are agreed with the outcomes of Larimi et al. [35], Shaw et al. [36], and Akabar and Batt [47].

The variations in flow resistance $(\bar{\lambda})$ to stenosis height for different values of heat source or sink constant (β), Grashof number (G_r), magnetic field constraint (M), and the volume flow rate (q) are depicted in Figs.8-11. It has been seen that the resistance to flow $(\bar{\lambda})$ increases with ascends in δ, M, and q, however, decreases with descends in β and G_r. From these figures, It is noticed that the flow resistance is less in the copper nanoparticles concentrated blood. It is worth mentioning the physical reason behind such observation. The obstructed fluid in the constriction region quickly moves towards the main flow region and hence the fluid enhances the resistance to the flow in the pre-stenotic region for a transitory period before attaining the minimum in the post stenotic region. A similar reason is attributed to the reduction in resistance in the post stenotic region. These findings predict that copper nanoparticles can improve blood flow and enhances the hemodynamic response. The wall shear stress (τ_h) against the axial distance (z) for different values of heat absorption constant(β), stenosis height (δ), Grashof number (G_r) , and magnetic field constraint (M) are plotted in Figs.12-15. It is seen that the wall shear stress (τ_h) is upturned with growth in δ and β while declines with growth in G_r and M. It is also perceived that the wall shear stress (τ_h) increases from $z = 0$ to $z = 0.26$ and from there it decreases to $z = 0.4$ and again, it increases to $z = 0.53$ from there it gradually decreases and approaches zero. Understanding the wall shear stress is very critical to find out the things which are happening with the small arteries and arterioles. The pressure gradient and the wall shear stress impact the arteries and these arteries become very firm over time, and they lose their elasticity. These affected arteries when exposed to high blood pressure leads to the rupture of the arterial wall. These results are in agreement with the numerical result of Ramana [44], Akbar [48] and are also holding good with experimental outcomes of Bureau et al. [50] and McMillan [51] in the case of resistance to the flow and wall shear stress of blood.

The trapping phenomenon is an essential part to study fluid flow issues. It is by and large the arrangement of the inside flowing bolus. The movement of the inside flowing bolus in a fluid is implanted by a different stream. This phenomenon is particularly useful in blood circulation issues. Streamlines have been plotted in Figs. 16 - 18 for pure-blood and Cu-blood for different values of β, δ, and M. It is observed that the size of the bolus increases with heat source constant (β), and stenosis height (δ), and magnetic field constraint (M). From Fig. 16-18, it is also noticed that the volume of the trapped bolus lessens for Cu nanoparticles concentrated blood as compared to pure blood.

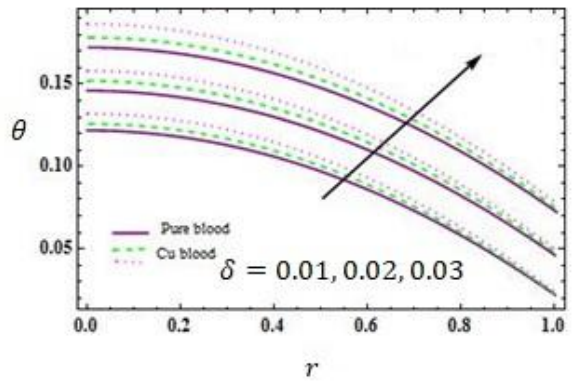

Fig. 2. Variations in temperature (θ) for δ when $d = 0.2, \mathrm{L}_0 = 0.4, \beta = 0.1, L = 1, z = 0.1$

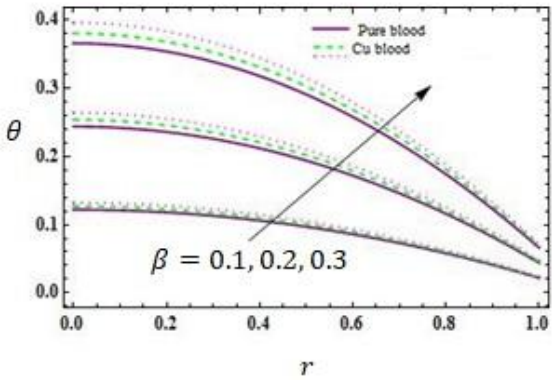

Fig. 3. Variations of temperature (θ) for β when $d = 0.2, \mathrm{L}_0 = 0.4, \delta = 0.01, L = 1, z = 0.1$

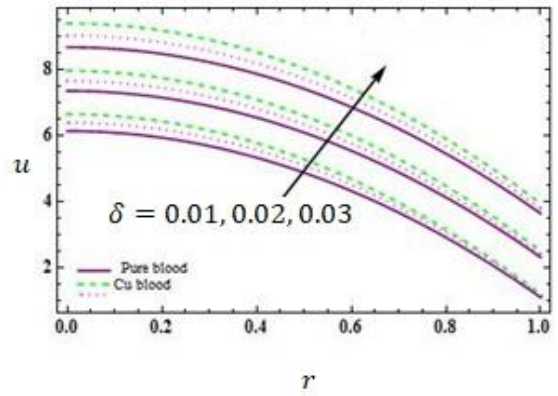

Fig. 4. Variations in velocity (u) for δ when $d = 0.2, \mathrm{L}_0 = 0.4, \beta = 0.1, L = 1, z = 0.1, \mathrm{Gr} = 2; M =$

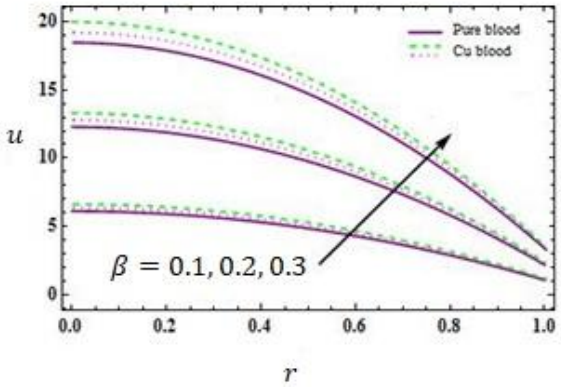

Fig. 5. Variations in velocity (u) for β when $d = 0.2, \mathrm{L}_0 = 0.4, \delta = 0.01, L = 1, z = 0.1, \mathrm{Gr} = 2; M = 0.$

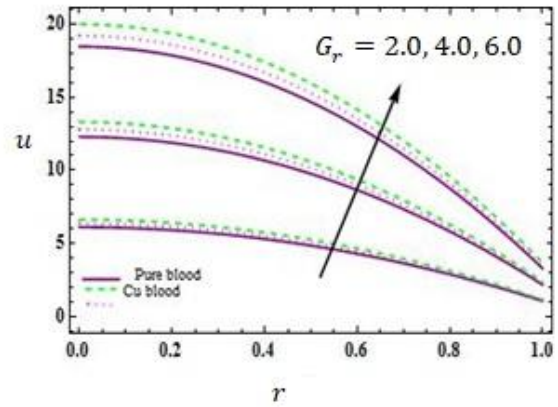

Fig. 6. Variations in velocity (u) for G_r when $d = 0.2, \mathrm{L}_0 = 0.4, \beta = 0.1, L = 1, z = 0.1, \delta = 0.01, M =$

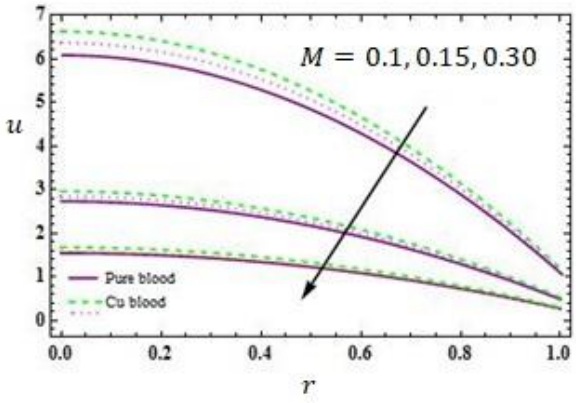

Fig. 7. Variations in velocity (u) for M when $d = 0.2, \mathrm{L}_0 = 0.4, \delta = 0.01, L = 1, z = 0.1, \mathrm{Gr} = 2, \beta =$

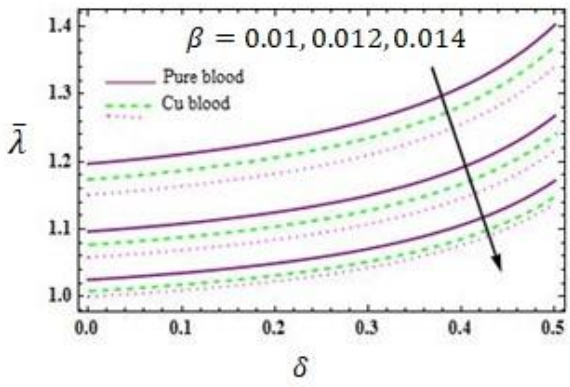

Fig. 8. Variations in flow resistance $(\overline{\lambda})$for β when $d = 0.2, \mathrm{L}_0 = 0.4, L = 1, q = 0.01, \mathrm{Gr} = 2, M = 0.1$

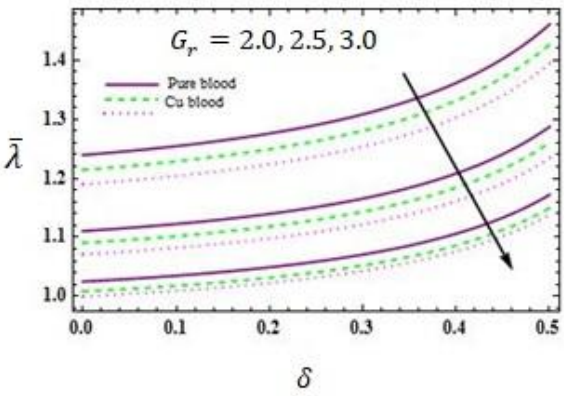

Fig. 9. Variations in flow resistance $(\overline{\lambda})$ for G_r when $d = 0.2, \mathrm{L}_0 = 0.4, L = 1, q = 0.01, \beta = 0.1, M = 0.1$

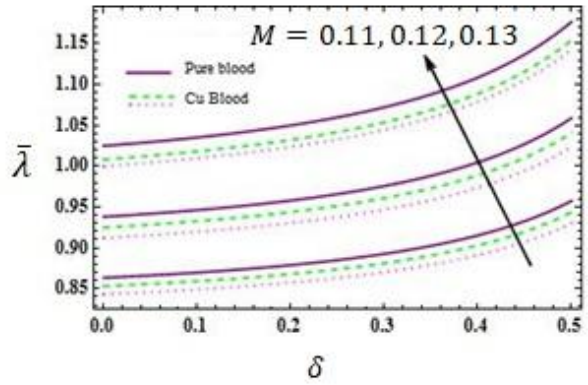

Fig. 10. Variations in flow resistance $(\overline{\lambda})$ for M when $d = 0.2, \mathrm{L}_0 = 0.4, L = 1, q = 0.01, \beta = 0.1, \mathrm{Gr} = 2$

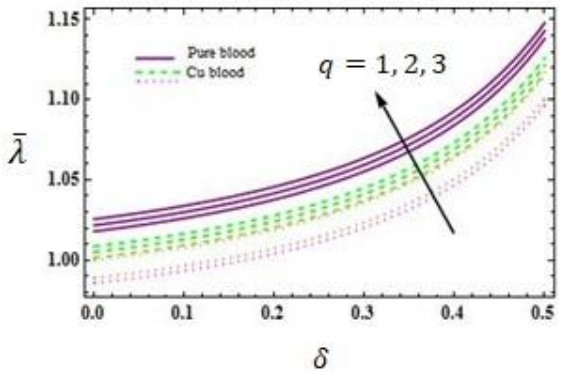

Fig. 11. Variations in flow resistance $(\overline{\lambda})$ for q when $d = 0.2, \mathrm{L}_0 = 0.4, L = 1, \beta = 0.1, M = 0.1$

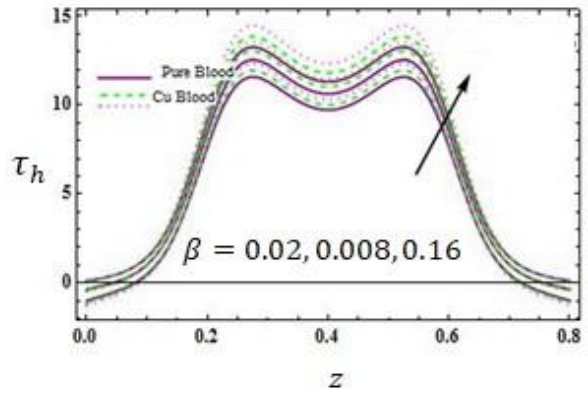

Fig. 12. Variations in wall shear stress (τ_h) for β when $d = 0.2, \mathrm{L}_0 = 0.4, L = 1, q = 1, \delta = 0.1, M = 1, \mathrm{Gr} = 2$

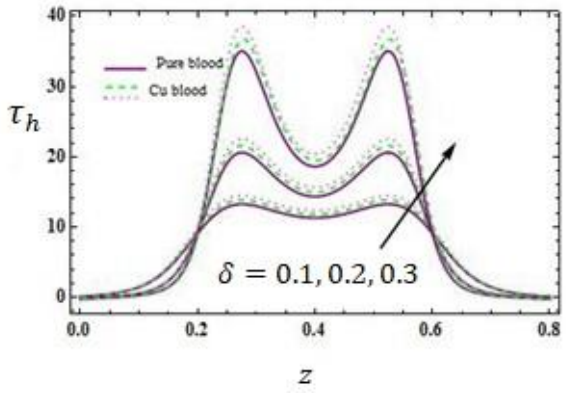

Fig. 13. Variations in wall shear stress (τ_h) for δ when $d = 0.2, \mathrm{L}_0 = 0.4, L = 1, q = 1, \beta = 0.02, M = 1, \mathrm{Gr} =$

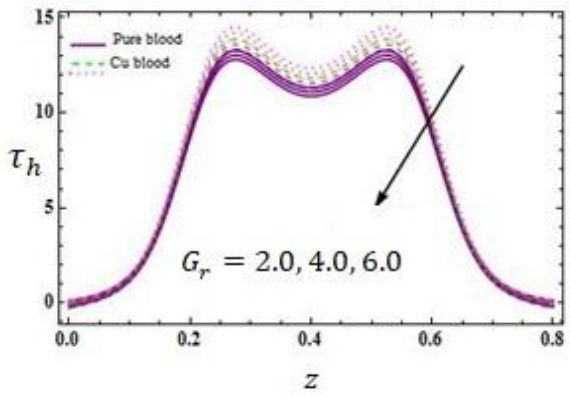

Fig. 14. Variations in wall shear stress (τ_h) for G_r when $d = 0.2, \mathrm{L}_0 = 0.4, L = 1, q = 1, \delta = 0.1, M = 1, \beta = 0.($

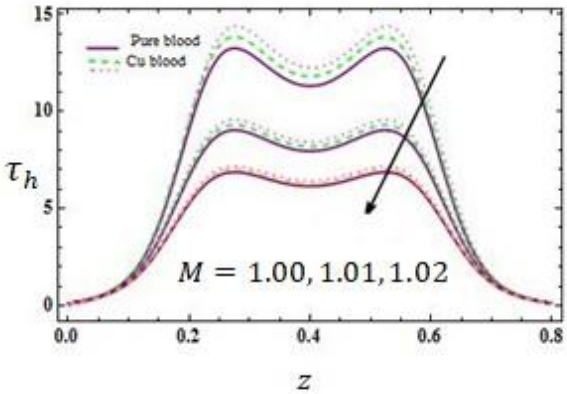

Fig. 15. Variations in wall shear stress (τ_h) for M when $d = 0.2, \mathrm{L}_0 = 0.4, L = 1, q = 1, \beta = 0.02, \delta = 0.1, \mathrm{Gr}$

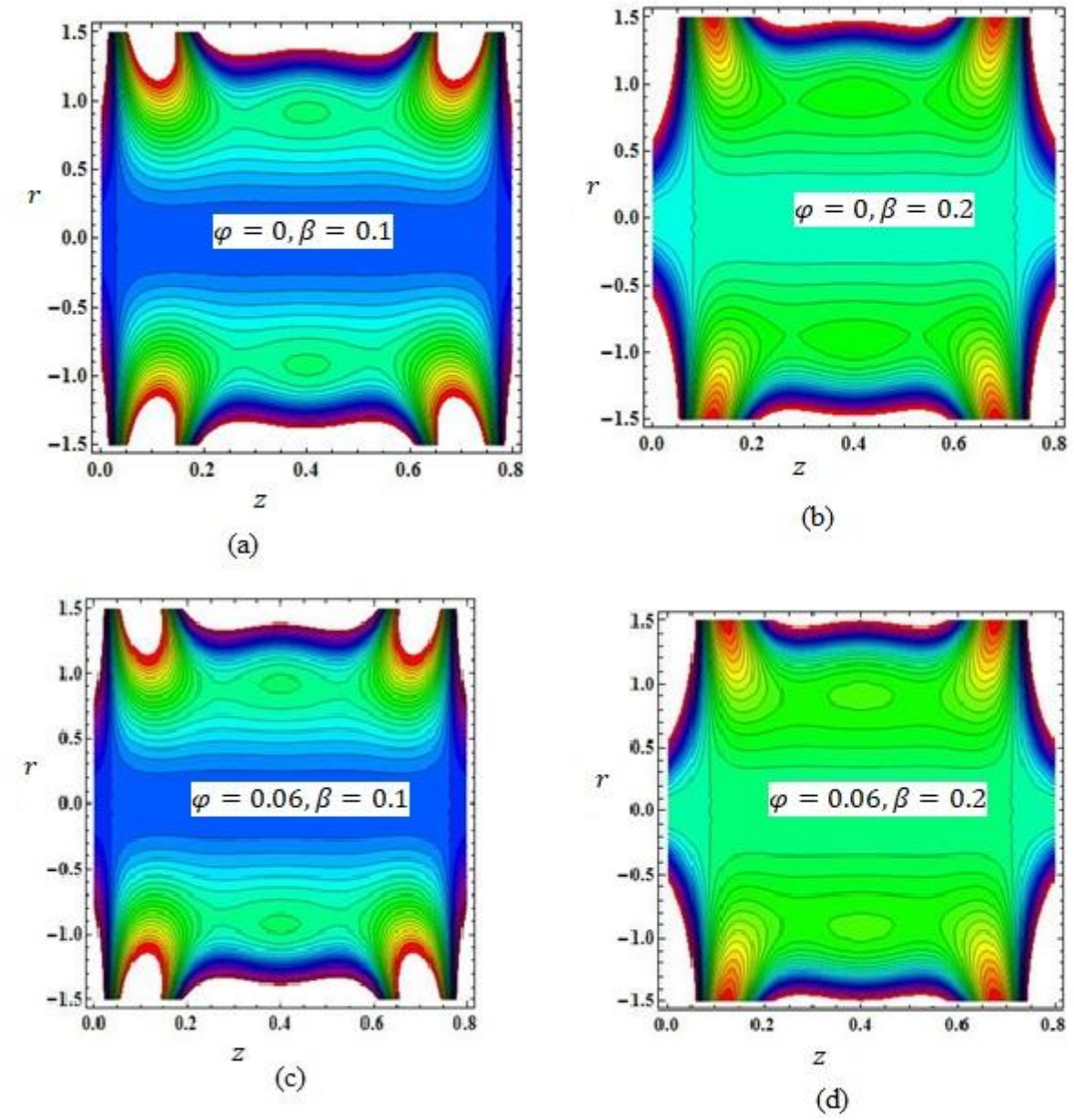

Fig. 16. Streamlines for pureblood $(\varphi = 0)$when (a) β =0.1 (b) β =0.2 and Cu nanoparticles concentrated blood $(\varphi = 0.06 \neq 0)$when (c) $\beta = 0.1$, (d) $\beta = 0.2$

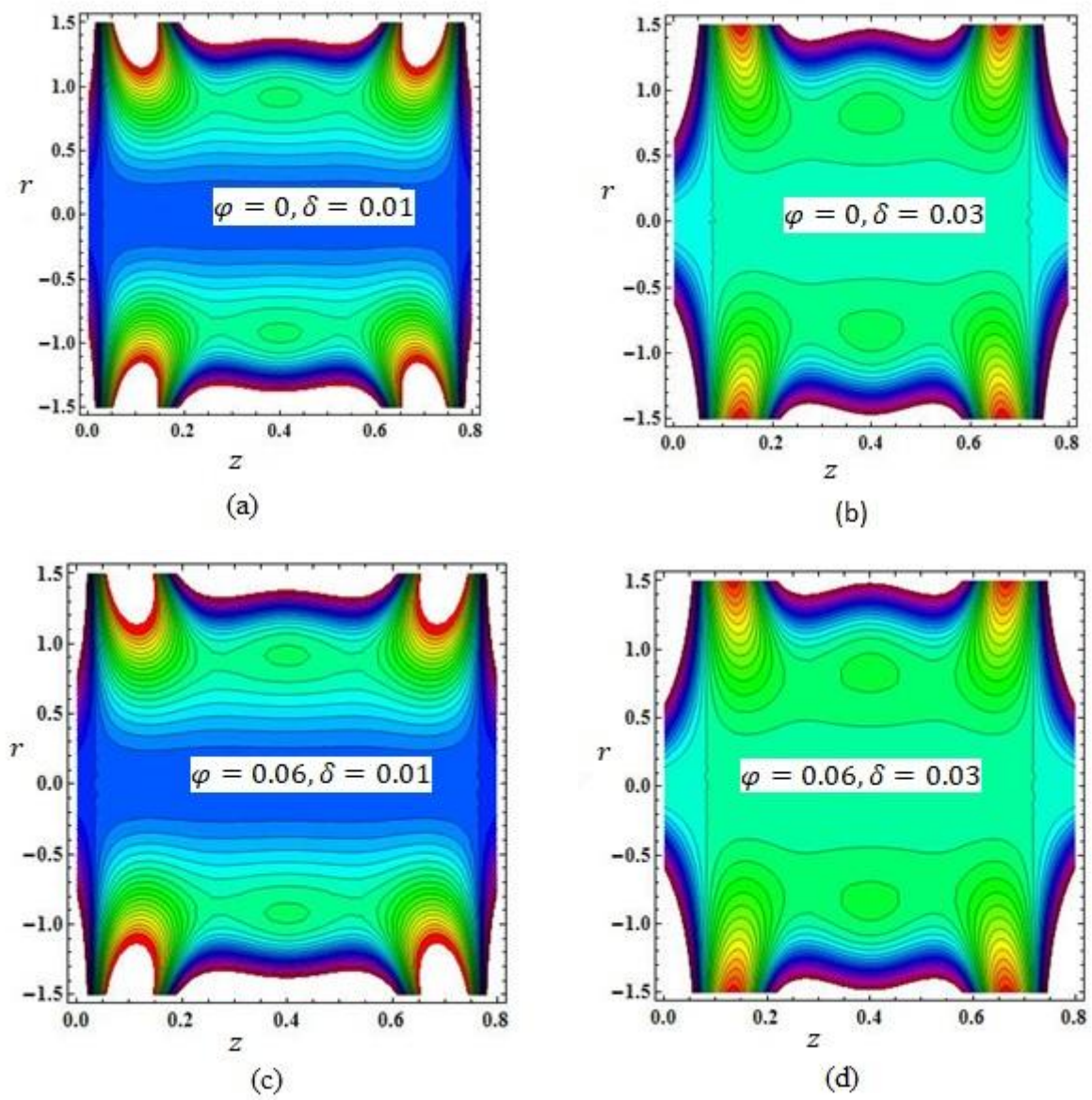

Fig. 17. Streamlines for pureblood $(\varphi = 0)$ when (a) $\delta = 0.01$ (b) $\delta = 0.03$ and Cu nanoparticles concentrated blood $(\varphi = 0.06 \neq 0)$ when (c) $\delta = 0.0.01$ (d) $\delta = 0.0.03$

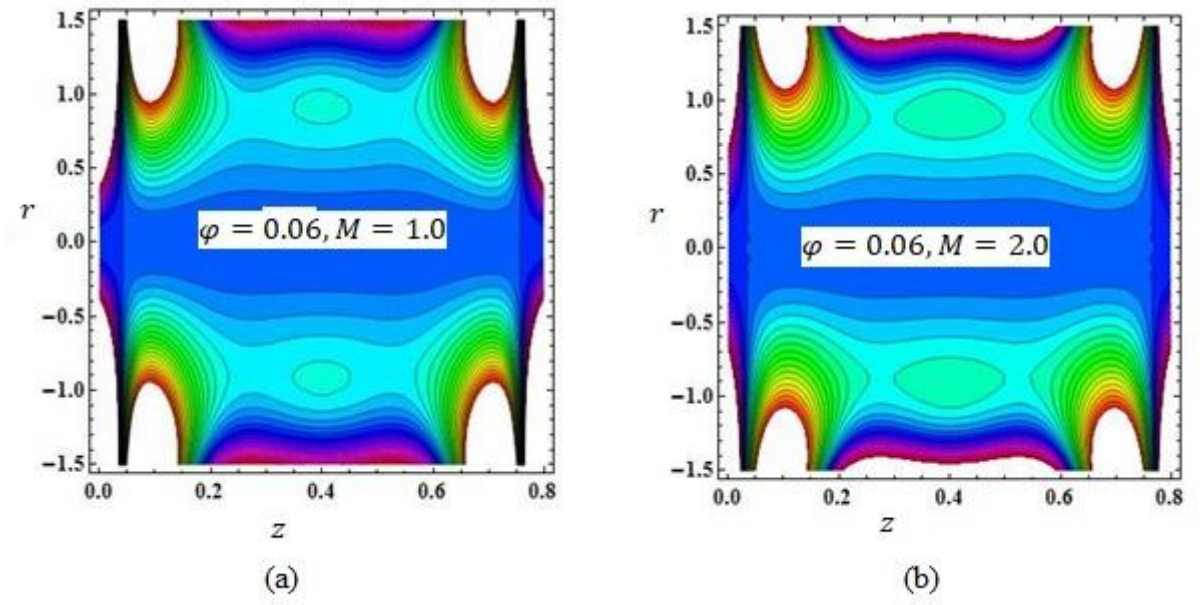

Fig. 18. Streamlines for Cu nanoparticles concentrated blood $(\varphi = 0.06 \neq 0)$when (a) $M = 1.0$ (b) $M = 2.0$

5. Conclusion

The present article is intended for investigating the impact of the magnetic field and copper nanoparticles on the flow of base fluid through an artery with overlapping stenosis. The key points of the present work are summarized below.

- The velocity profile increases with the height of stenosis (δ), heat absorption constant (β), and Grashof number (G_r) but decreases with magnetic field constraint (M).
- The flow resistance $(\bar{\lambda})$ rises with ascends in δ, M, and q but it falls with an increase in β and G_r.
- The wall shear stress (τ_h)increases with growth in stenosis height and heat absorption constant and however decreases with growth in Grashof number and magnetic field constant.
- The temperature (θ) rises when the stenosis height and heat absorption constant increase and the temperature is maximum at the center of the tube and least near the walls of the tube.
- The volume of trapped bolus increases for pure blood and copper blood an increase in the heat source constant and stenosis height. However, the size of the trapped bolus is more for pureblood as compared to copper nanoparticle's concentrated blood.

Acknowledgment

The authors are thankful to the reviewer(s) for their valuable comments and suggestions to improve the quality of the work.

References

[1] A. S. Popel, P. C. Johnson, Microcirculation and hemorheology, Annu Rev Fluid Mech. 37 (2005) 43–69.

[2] H. H. Lipowsky, Microvascular rheology and hemodynamics, Microcirculation, 12 (2005) 5–15.

[3] J. B. Freund, Numerical simulation of flowing blood cells, Annu. Rev. Fluid Mech. 46 (2014) 67–95.

[4] M. Sharan, A. S. Popel, A two-phase model for flow of blood in narrow tubes with increased effective viscosity near the wall, Biorheology. 38 (2001) 415–28.

[5] S. Chien, S. Usami, H. M. Taylor, J. L. Lundberg, M. I. Gregersen, Effects of hematocrit and plasma proteins on human blood rheology at low shear rates, J. Appl. Physiol. 21 (1966) 81–87.

[6] L. Zixiang, Z. Yuanzheng, R. R. Rao, R. Clausen, K. C. Aidun, Nanoparticle transport in cellular blood flow, Comp. Fluids. 172 (2018) 609-620.

[7] G. B. Thurston, Frequency and shear rate dependence of viscoelasticity of human blood, Biorheology. 10 (1973) 375–381.

[8] A. Apostolidis, A. Beris, Modeling of the blood rheology in steady-state shear flows, J. Rheol. 58 (2014) 607–633. doi:10.1122/1.4866296.

[9] D. Quemada, A non-linear Maxwell model of biofluids: Application to normal human blood, Biorheology. 30 (1993) 253– 265.

[10] M. C. Williams, J. S. Rosenblatt, D. S. Soane, Theory of blood rheology based on a statistical mechanics treatment of rouleaux, and comparisons with data, Int. J. Polym. Mater. 21 (1993) 57–63.

[11] G. Vlastos, D. Lerche, B. Koch, The superposition of steady on oscillatory shear and its effect on the viscoelasticity of human blood and a blood-like model fluid, Biorheology. 34 (1997) 19–36.

[12] Y. Dimakopoulos, A. Bogaerds, P. Anderson, M. Hulsen, F.P.T. Baaijens, Direct numerical simulation of a 2D idealized aortic heart valve at physiological flow rates, Comp. Meth. Biomech. and Biomed. Eng. 15(11) (2012) 1157–1179.

[13] M. Anand, K. R. Rajagopal, A shear-thinning viscoelastic fluid model for describing the flow of blood, Int. J. Cardiovascular Med. Sc. 4(2) (2004) 59–68.

[14] K. R. Rajagopal, A. R. Srinivasa, A thermodynamic frame work for rate type fluid models, J. Non-Newtonian Fluid Mech. 80 (2000) 207–227.

[15] T. Bodnar, A. Sequeira, Numerical study of the significance of the non-Newtonian nature of blood in steady flow through a stenosed vessel, Advances in mathematical fluid mechanics. Springer; (2010) 83–104.

[16] D. Chakraborty, M. Bajajb, L. Yeob, J. Friendb, M. Pasquali, J. R. Prakash, Viscoelastic flow in a two-dimensional collapsible channel, J. Non-Newtonian Fluid Mech. 165 (2010) 1204–1218.

[17] S. Rodbard, Dynamics of Blood flow in stenotic lesions, American Heart J. 72(5) (1966) 698-704.
[18] D. F. Young, Effect of time-dependent stenosis on flow through a tube, Trans. ASME J. Engng Ind. 90 (1968) 248-254.
[19] J. C. Misra, M. K. Patra, S. C. Misra, A non-Newtonian fluid model for blood flow through arteries under stenotic conditions, J. Biomech. 26(9) (1993) 1129-1141.
[20] S. Chakravarty, P. K. Mandal, Mathematical modeling of blood flow through overlapping arterial stenosis, Math. Comput. Model. 19 (1994) 59-70.
[21] R. Ponalagusamy, Two-Fluid Model for Blood Flow through tapered arterial stenosis: Effect of Non-zero Couple Stress Boundary Condition at the Interface, Int. J. Appl. Comput. Math. 3 (2017) 807-824.
[22] J. V. RamanaReddy, D. Srikanth, Impact of blood vessels wall flexibility on the temperature and concentration dispersion, J. Appl. Comput. Mech. 6(3) (2020) 564-581.
[23] M. K. Sahu, S. K. Sharma, A. K. Agarwal, Study of arterial blood flow in a stenosed vessel using non-Newtonian couple stress fluid model, Int. J. Dynamic. Fluids, 6(2) (2010) 248-257.
[24] S. Nadeem, N. S. Akbar, T. Hayat, A. Hendi, Power-law fluid model for blood flow through a tapered artery with a stenosis, Appl. Math. Comput. 217 (2011) 7108–7116.
[25] Y. Dimakopoulos, G. Kelesidis, S. Tsouka, G. C. Georgiou, J. Tsamopoulos, Hemodynamics in stenotic vessels of small diameter under steady state conditions: Effect of vescoelasticity and migration of red blood cells, Biorheology. 52 (2015) 183-210.
[26] Z. Ismail, A. Ilyani, M. Norzieha, A. Norsarahaida, A power –Law Model of blood through a tapered overlapping stenosed artery, Appl. Math. Comput. 195(2) (2008) 669-680.
[27] V. P. Srivastava, S. Mishra, Non-Newtonian arterial blood flow through overlapping stenosis, Appl. Appl. Math. 5(1) (2010) 225-238.
[28] G. C. Shit, S. Maiti, M. Roy, J. C. Misra, Pulsatile flow and heat transfer of blood in an overlapping vibrating atherosclerotic artery: A numerical study, Math. Comput. Simul. 166 (1) (2019) 432-450.
[29] S. U. S.Choi, J. A. Eastman, Enhancing thermal conductivity of fluids with nanofluids, ASME Fluids Engg. Div. 231 (1995) 99-105.
[30] J. Buongiorno, Convective transport in nanofluids, J. Heat Trans. 128(3) (2006) 240-250. http://dx.doi.org/10.1115/1.2150834
[31] K. Vajravelu, K. V. Prasad, J. Lee, C. Lee, I. Pop, R.A.V. Gorder, Convective heat transfer in the flow of viscous Ag-blood and Cu-water nanofluids over a stretching surface, Int. J. Therm. Sci. 50 (2011) 843.
[32] M. Gudekote, D. Baliga, R. Choudhari, H. Vaidya, K. V. Prasad, O. D. Makinde, Influence of variable viscosity and wall properties on the peristalsis of Jeffrey fluid in

a curved channel with the radial magnetic field, Int. J. Thermofluids. Sci. Tech. 7(2) (2020) 1-16. https://doi.org.10.36963/IJTST.2020070203

[33] G. Sankad, M. Dhange, Effect of chemical reactions on the dispersion of a solute in the peristaltic motion of Newtonian fluid with wall properties, Malaysian J. Math. Sci. 11(3) (2017) 347-363.

[34] M. K. Nayak, A. K. Abdu-Hakeem, B. Ganga, Influence of non-uniform heat source/sink and variable viscosity on mixed convection flow of third grade nanofluid over an inclined stretched Riga plate, Int. J. Thermofluids. Sci. Tech. 6(4) (2019) 1-28. https://doi.org.10.36963/IJTST.19060401

[35] M. M. Larimi, A. Ramiar, A. A. Ranjbar, Numerical simulation of magnetic nanoparticles targeting in a bifurcation vessel, J. Magn. Magn. Mater. 362 (2014) 58-71.

[36] S. Shaw, P. V. S. N. Murthy, P. Sibanda, Magnetic drug targeting in a permeable microvessel, Microvasc. Res. 85 (2013) 77-85.

[37] A. Rahbari, M. Fakour, A. Hamzehnezhad, M. A. Vakilabadi, D. D. Ganji, Heat transfer and fluid flow of blood with nanoparticles through porous vessels in a magnetic field: A quasi-one-dimensional analytical approach, Math. Biosc. 283 (2017) 38-47.

[38] M. Hatami, J. Hatami, D. D. Ganji, Computer simulation of MHD blood conveying gold nanoparticles as a third grade non-Newtonian nanofluid in a hollow porous vessel, Comput. Meth. Prog. Bio. 113(2) (2014) 632-641.

[39] M. J. Uddin, A. K. Fazlul-Hoque, M. M. Rahman, K. Vajravelu, Numerical simulation of convective heat transport within the nanofluid filled vertical tube of plain and uneven sidewalls, Int. J. Thermofluids. Sci. Tech. 6(1) (2019) 1-24. https://doi.org.10.36963/IJTST.19060101

[40] M. K. Nayak, HHR impact on 3D radiative stretched flow of Cu-H_2O nanofluid influenced by the variable magnetic field and convective boundary condition, Int. J. Thermofluids. Sci. Tech. 6(1) (2019) 1-23. https://doi.org.10.36963/IJTST.19060101

[41] T. Islam, N. Parveen, Md.Fayaz-al-Asad, Hydromagnetic natural convection heat transfer of copper-water nanofluid within a right-angled triangular cavity, Int. J. Thermofluids. Sci. Tech. 7(3) (2020) 1-18. https://doi.org.10.36963/IJTST.2020070304

[42] S. Molli, K. Naikoti, MHD Natural convective flow of Cu-water nanofluid over a past infinite vertical plate with the presence of time-dependent boundary condition, Int. J. Thermofluids. Sci. Tech. 7(3) (2020) 1-18. https://doi.org.10.36963/IJTST.2020070304

[43] N. S. Akbar, Endoscope effects on the peristaltic flow of Cu-water nanofluids, J. Comput. Theor. Nanosci. 11 (2014) 1150-1155.

[44] J. V. Ramana, D. Srikanth, D. Samir, K. Das, Modelling and simulation of temperature and concentration dispersion in a couple stress nanofluid flow through stenotic tapered arteries, Eur. Phys. J. Plus. 132(8) (2017) 365.

[45] S. Nadeem, S. Ijaz, Nanoparticles analysis on the blood flow through a tapered catheterized elastic artery with overlapping stenosis, Eur. Phys. J. Plus. 129(11) (2014) 249.

[46] T. Elnaqeeb, K. S. Mekheimer, F. Alghamdi, Cu-blood flow model through a catheterized mild stenotic artery with a thrombosis, Math. Biosci. 282 (2016) 135-146.

[47] N. S. Akbar, A. W. Butt, Magnetic field effects for copper suspended nanofluid venture through a composite stenosed artery with permeable walls, J. Magn. Magn. Mater. 381 (2015) 285-291.

[48] N. S. Akbar, Metalic nanoparticle analysis for the blood Flow in tapered stenosed arteries: Application in nanomedicines, Int. J. Bio. Math. 9(1) (2016) 1-18. https://doi.org/10.1142/S1793524516500029

[49] B. C. Pak, Y. I. Cho, Hydrodynamic and heat transfer study of dispersed fluids with submicron metallic oxide particles, Exp. Heat Transf. 11(2) (1998) 151-170.

[50] M. Bureau, J. C. Healy, D. Bourgoin, M. Joly, L. D. Biophysique, F. D. Medecine, P. Salpetriere, Rheological hysteresis of blood at low shear rate, Biorheology, 16 (1979) 7-100.

[51] D. E. McMillan, J. Strigberger, N. G. Utterback, Rapidly recovered transient flow resistance: A newly discovered properties of blood, AM. J. Physiol. Hear. Circ. Physiol. 253 (1987) 919-926.